J. Phys.: Condens. Matter **12** (2000) 9761–9770. Printed in the UK PII: S0953-8984(00)15765-0

Phase separation, thermal history and magnetic behaviour of Sr doped $LaCoO_3$

G Baio†, G Barucca†, R Caciuffo†, D Rinaldi†, J Mira ‡, J Rivas ‡, M A Señarís-Rodríguez§ and D Fiorani‖

†Istituto Nazionale per la Fisica della Materia and Dipartimento di Scienze dei Materiali, Universitá di Ancona, I-60131 Ancona, Italy

‡Departamento de Física Aplicada, Universidade de Santiago, E-15706 Santiago de Compostela, Spain

§Departamento de Química Fundamental e Industrial, Universidade de A Coruña, E-15008 A Coruña, Spain

‖Istituto di Chimica dei Materiali, Consiglio Nazionale delle Ricerche, Casella Postale 10, I-00010 Monterotondo Stazione, Roma, Italy

Received 24 July 2000, in final form 26 September 2000

Abstract. High-resolution transmission electron microscopy observations and magnetic ac susceptibility measurements have been carried out to study the changes in the magnetic properties of $La_{1-x}Sr_xCoO_3$ samples ($x \leqslant 0.3$) processed at different annealing temperatures, ranging from 1273 to 1573 K. Although neutron diffraction excludes the coexistence of distinct phases with different chemical composition, room temperature micrographs taken along the $[0, -1, 1]$ rhombohedral zone-axis show bright fringes of different widths, extending over regions with sizes ranging from 8 to 40 nm. These regions are detected in all the samples, whatever the Sr content or the annealing temperature T_a. However, their number depends strongly on the processing conditions and becomes smaller and smaller as T_a increases. The periodicity of the bright fringes cannot be accounted for, either by variations in the sample thickness or by crystallographic defects, but it can be simulated if the presence of aperiodically alternate Sr-rich and La-rich (0, 1, 1) planes is assumed. On the other hand, the susceptibility measurements show that the amount of ferromagnetic phase present in each specimen depends on its thermal history. This suggests that the segregation of a second electronic phase takes place, the nucleation of which is influenced by the spatial homogeneity of the dopant distribution.

1. Introduction

The discovery that in mixed-valent manganites a huge variation of electrical resistivity can be induced by a small, external magnetic field (colossal magnetoresistance) [1, 2] has raised a great deal of attention on perovskite systems. Colossal magnetoresistance (CMR) arises from competition between metal and insulator states and recently Uehara *et al* have demonstrated that percolative phase separation underlies this interesting phenomenon [3]. Using transmission electron microscopy (TEM) to study the microstructure of the $La_{1-x-y}Pr_yCa_xMnO_3$ system, these authors demonstrated the coexistence of a charge-ordered, insulating phase and a charge-disordered, ferromagnetic-metallic phase, over a broad range of the Pr : La ratio. This coexistence is not simply due to chemical inhomogeneity. By a combination of techniques Uehara *et al* [3] were able to exclude the presence of chemical phases with different composition. On the other hand, the length scale of the phase separation they observed (hundreds of nanometres) was too large to be due to electronic charge segregation into magnetic

0953-8984/00/479761+10$30.00

clusters. A number of studies addressing the nature of this electronic phase separation in manganites have already appeared [4–7].

Another perovskite system where magnetic properties, structural distortions and electrical transport behaviour are intricately entangled is $La_{1-x}Sr_xCoO_3$. Changes of the cobalt spin configuration with temperature and Sr concentration give a rich variation of magnetic and transport properties that has attracted considerable interest over the last four decades [8–17]. Moreover, a large negative magnetoresistance ratio has been observed [18, 19] for low Sr doping, that appears to be analogous to the CMR found in some manganese perovskites.

At a low temperature, the parent compound $LaCoO_3$ is a diamagnetic insulator, the Co^{3+} ions being all in the low spin $^1A_1$ state ($S = 0$). Thermal excitation of higher spin configurations takes place above $\approx$ 90 K [9, 17]. Substitution of Sr^{2+} for La^{3+} stabilizes an intermediate spin state ($S = 1$), and ferromagnetism appears in Sr^{2+}-rich clusters, coexisting with a paramagnetic $LaCoO_3$-like matrix [11, 20, 21]. At low doping ranges, $x < 0.1$, a freezing of the magnetic moments into a spin–glass phase has been proposed [17, 22]. In the range $0.1 \leqslant x < 0.2$, the intermediate spin (IS) clusters become larger, and superparamagnetic below a Curie temperature $T_C \approx 230$ K. A collective freezing of the cluster magnetic moments at a temperature $T_g < T_C$ is suggested by the observation of spin–glass-like characteristics in the magnetization and susceptibility curves [23]. For higher Sr content, $x > 0.20$, the ferromagnetic clusters reach a percolation threshold, and the system shows bulk ferromagnetism below $T_C \approx 230$ K [24].

On the basis of ac magnetic susceptibility and magnetization measurements, Anil Kumar *et al* proposed that the origin of the unusual magnetic behaviour reported for $La_{1-x}Sr_xCoO_3$ [11, 24] must be searched for in the presence of compositional inhomogeneity, rather than attributed to a dependence of the cluster-size upon temperature and doping level [25]. They showed that the magnetic properties are strongly influenced by the processing conditions and that a well-defined spin glass behaviour is obtained, for $x < 0.18$, only for samples annealed at $T \geqslant 1500$ K. Earlier high resolution TEM observations have given, in fact, direct evidence for an inhomogeneous distribution of the Sr^{2+} ions, and the segregation of the material into hole-rich ferromagnetic regions embedded in a hole-poor semiconducting matrix [22]. However, neutron diffraction studies do not show any indication of two phases with different chemical composition extending over macroscopic regions [22, 26]. A simple chemical phase separation does not seem sufficient to explain the complex magnetic and transport properties of the system.

To obtain more information on this intricate subject, we have carried out new experiments on $La_{1-x}Sr_xCoO_3$ samples ($x \leqslant 0.3$) processed at different annealing temperatures. Using high-resolution transmission electron microscopy and ac susceptibility measurements, we show that the amount of ferromagnetic material present depends on the thermal history, but we argue that an electronic phase segregation is accomplished as a result of dynamic, cooperative oxygen displacements.

2. Experimental details

$La_{1-x}Sr_xCoO_3$ samples ($x = 0.10$, 0.15, 0.20, 0.25 and 0.30) were prepared by a co-precipitation method from La_2O_3, $Co(NO_3)_2{\cdot}6H_2O$ and $SrCO_3$ as starting materials [11]. The cobalt nitrate was first dissolved in water and the cobalt content in the solution was determined gravimetrically with anthranilic acid as precipitating agent. Known volumes of the cobalt solution were then mixed with corresponding lanthanum and strontium nitrate solutions, obtained by dissolving in nitric acid weighted amounts of dry La_2O_3 and $SrCO_3$. Co-precipitation at pH 11 was achieved by adding aqueous solutions of KOH and K_2CO_3 as precipitating agents. The precipitates were carefully washed, dried, and then decomposed at

1023 K. The obtained precursor powders were pressed into pellets, heated in air for 24 hours at different temperatures (T_a = 1273, 1373, 1473 and 1573 K), and then cooled very slowly to room temperature (at 0.3 K min^{-1} down to 973 K and at 0.7 K min^{-1} thereafter).

The product materials were examined by x-ray powder diffraction with a Philips PW 1729 diffractometer and Cu Kα = 1.5418 Å radiation. NaCl was used as an internal standard. All the samples were single-phase materials. The thermal stability of all the materials was checked by differential thermal analysis and thermogravimetric analysis, with a Perkin–Elmer system. Iodometric titrations were carried out to analyse the oxygen content of the materials. The samples were dissolved in acidified KI solutions, and the I_2 generated was titrated against a thiosulphate solution. The whole process was carried out under a nitrogen atmosphere. The iodometric titrations revealed that the samples are stoichiometric in oxygen. Particle size and morphology of the samples annealed at 1273 K were studied with a JEOL 6400 SEM microscope. The co–precipitated samples showed individual particles with quite perfect spherical shapes with sizes between 700 and 900 nm.

High-resolution transmission electron microscopy observations were carried out with a Philips CM200 microscope offering a point to point resolution of 0.27 nm. The samples were prepared by depositing the powder material on a carbon-coated copper grid.

Real and imaginary components of the external complex ac magnetic susceptibility were measured as a function of temperature with a Lake Shore 7000 system, using a mutual inductance technique. The calibration was performed using a $Gd_2(SO_4)_3{\cdot}8H_2O$ paramagnetic standard with the same shape and size as the investigated samples. Demagnetizing effects have been taken into account in the calculation of the so called internal susceptibility. Data were collected on warming from 13 to 300 K, after zero field cooling of the sample, with a driving field of amplitude H_0 = 3.75 Oe, oscillating at a frequency of 1 kHz. The temperature of the sample was controlled with an accuracy of about 0.1 K.

3. Results

The real part of the linear magnetic ac susceptibility, χ', measured for $x = 0.10$ samples annealed at T_a = 1273 and 1373 K, is shown as a function of temperature in figure 1. For the sample annealed at 1273 K, an onset of the signal is observed at about 240 K. Ferromagnetic order with a correlation length of about 600 Å, and an ordered moment $\mu_0 = 0.3(1)\mu_B$ at T = 2 K, has been observed on the same sample by neutron diffraction [22]. The small value of the ordered moment suggests that the ferromagnetic phase occupies only a fraction of the total volume. This is consistent with the lack of a sharp transition at $\approx$ 240 K in the χ' curve, which also suggests a distribution of T_C values in the ferromagnetic regions. The maximum in the susceptibility, at around 60 K, has been attributed to spin–glass-like freezing in the volume of the material that is not ferromagnetic, consisting of superparamagnetic sized clusters. Annealing at higher temperatures suppresses the ferromagnetic transition, and a cusp-shaped susceptibility curve is obtained, with a maximum at 34 K. Although the shape of this curve is similar to that of a spin–glass system, no frequency dependence of the maximum position has been observed in the range of frequency between 1 and 10^4 Hz. The lack of frequency dependence indicates that the clusters' moments are strongly coupled between themselves and with the ferromagnetic regions.

The evolution of the magnetic susceptibility with annealing temperature for the samples with higher Sr content is shown in figures 2 and 3. For $x = 0.15$, the changes in the magnetic behaviour are similar to those observed for $x = 0.10$. The magnetic transition below 240 K becomes gradually less evident as T_a increases, until a cusp-shaped curve with a maximum at 65 K is obtained for T_a = 1573 K. For the sample annealed at T_a = 1273 K, neutron diffraction

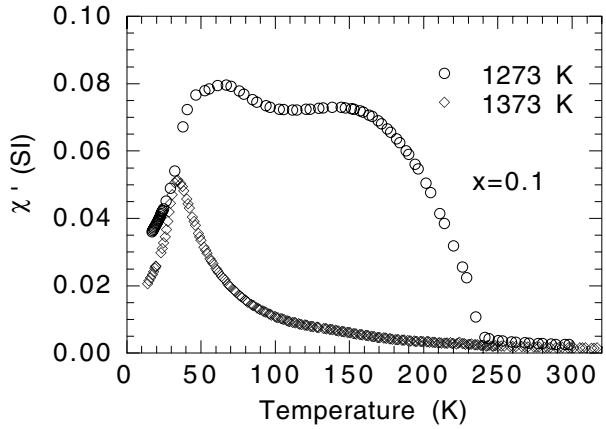

Figure 1. Real part (χ') of the linear magnetic ac susceptibility versus temperature of $La_{0.90}Sr_{0.10}CoO_3$ annealed for 24 h at 1273 and 1373 K. The data were taken with a driving field of amplitude H_0 = 3.75 Oe, oscillating at a frequency of 1 kHz.

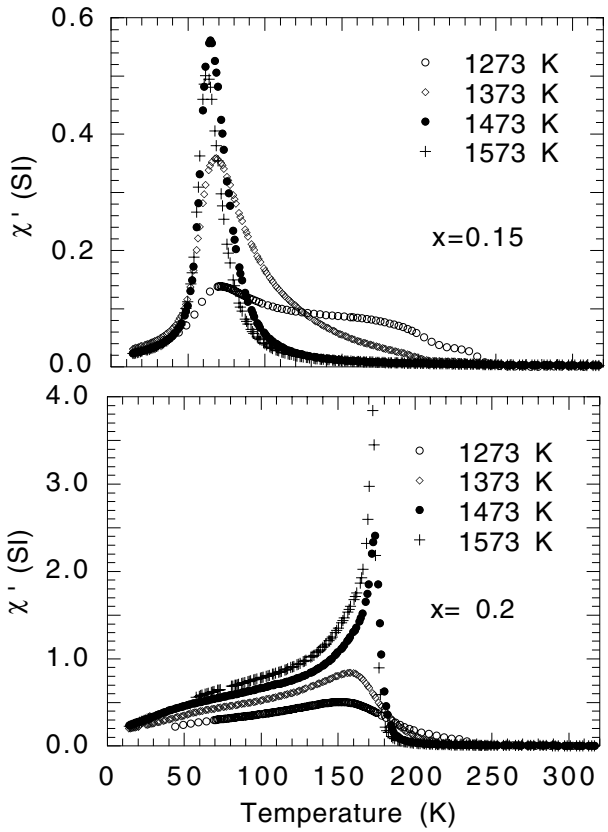

Figure 2. Real part (χ') of the linear magnetic ac susceptibility versus temperature of (a) $La_{0.85}Sr_{0.15}CoO_3$ and (b) $La_{0.80}Sr_{0.20}CoO_3$, annealed for 24 h at different temperatures, from 1273 to 1573 K. The data were taken with a driving field of amplitude H_0 = 3.75 Oe, oscillating at a frequency of 1 kHz.

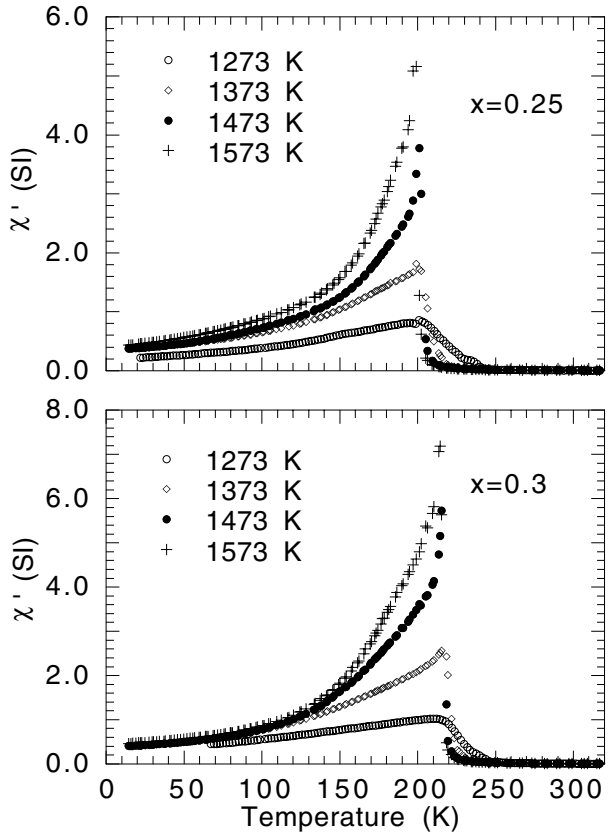

Figure 3. Real part (χ') of the linear magnetic ac susceptibility versus temperature of (a) $La_{0.75}Sr_{0.25}CoO_3$ and (b) $La_{0.70}Sr_{0.30}CoO_3$, annealed for 24 h at different temperatures, from 1273 to 1573 K. The data were taken with a driving field of amplitude H_0 = 3.75 Oe, oscillating at a frequency of 1 kHz.

showed the occurrence of ferromagnetic order below T_C = 230 K, with a correlation length of about 700 Å and an ordered moment $\mu_0 = 0.52(1)\mu_B$, at T = 2 K [22]. Now we see that the fraction of material ferromagnetically ordered becomes smaller and smaller with increasing annealing temperature, until a spin–glass-like behaviour is obtained. In fact, the position of the maximum susceptibility for the $x = 0.15$ sample annealed at T_a = 1573 K is frequency dependent, with a dynamic behaviour similar to that characterizing canonical spin–glasses. In particular, from the frequency dependence of the susceptibility maximum, a critical slowing down of the relaxation time was derived, with a critical exponent $\alpha = 6.4$ and a prefactor $\tau_0 = 8 \times 10^{-10}$. For canonical spin–glasses, a critical exponent $\alpha = 7$ is expected.

The change of the magnetic response with annealing temperature is different for samples with $x \geqslant 0.20$. As T_a increases, the shape of the susceptibility curve resembles more and more that of a typical ferromagnet. Going from T_a = 1273 K to T_a = 1573 K, the transition temperature shifts towards 220 K, whilst the magnitude of the susceptibility at T_C increases continuously. For the samples annealed at T_a = 1273 K, neutron diffraction has given a low-temperature ordered moment increasing from $1.26(5)\mu_B$, for $x = 0.20$, up to $1.71(2)\mu_B$, for $x = 0.30$.

The variation of the magnetic behaviour is accompanied by microstructural changes that

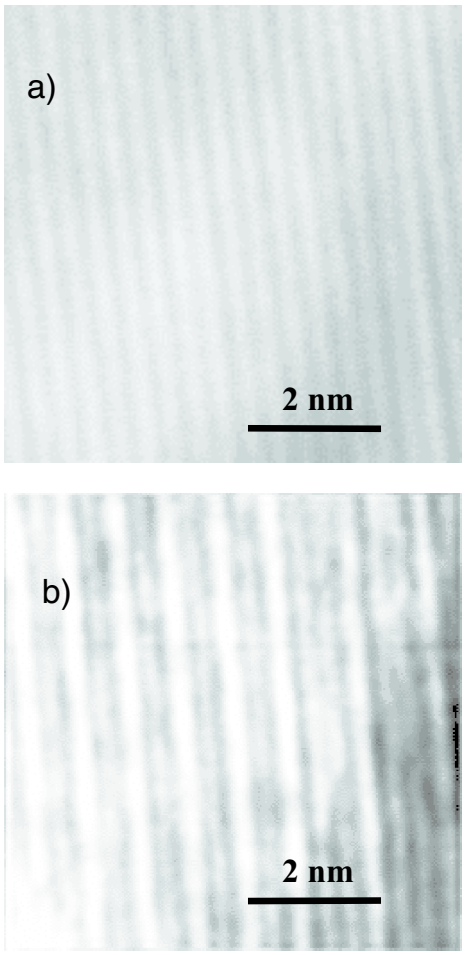

Figure 4. High resolution electron microscopy images taken along the [0, −1, 1] zone axis for the $La_{0.85}Sr_{0.15}CoO_3$ sample annealed at 1373 K. Panels (a) and (b) correspond to adjacent regions of the same crystallite. The different periodicity of the bright fringes indicates a non-homogeneous distribution of the Sr ions.

are easily detected by high-resolution electron microscopy (HREM). Figure 4 shows room temperature micrographs taken for the sample with $x = 0.15$ ($T_a = 1373$ K) along the [0, −1, 1] zone-axis (Miller indices refer to the rhombohedral crystallographic cell). Regions where bright fringes of different widths can be observed along the [−1, 1, 1] direction are present. The fringes' periodicity is non-uniform and varies from microcrystal to microcrystal in the same sample (figures 4(a) and (b)). The bright fringe regions with sizes ranging from 8 to 40 nm were detected in all the samples, whatever the Sr content or the annealing temperature. Only their number was found to be strongly dependent on the processing conditions, becoming smaller and smaller as T_a increases. Their presence and their spatial distribution cannot be accounted for either by variations in the sample thickness or by crystallographic defects. As shown by image simulations, the fringes could indicate the existence of aperiodically alternate Sr-rich and La-rich (0, 1, 1) planes.

An example of such a simulation, performed with the software package described in [27], is shown in figure 5. Once the crystal structure and the experimental conditions (sample orientation and absorption, electron beam energy and convergence, spherical and chromatic aberration coefficients) are assigned, the software package uses the so-called multi-slice method to calculate the electron density distribution at the exit face of the crystal [27]. The

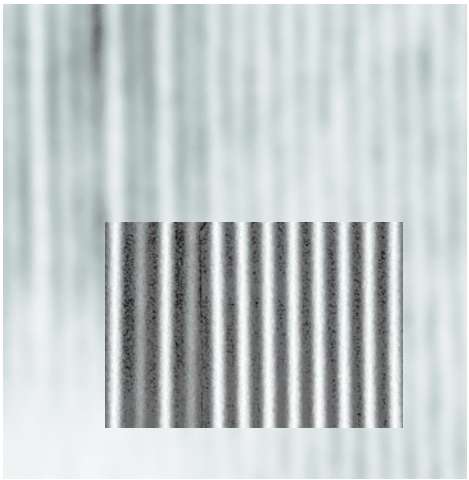

Figure 5. Simulation of the bright fringes' periodicity by aperiodically alternate Sr-rich and La-rich (0, 1, 1) planes.

sample is, ideally, sliced perpendicular to the direction of observation, and a phase grating is created by projecting the potential within each slice into a plane. Successive phase-object functions modify the incoming wave and propagate it between the slices. Different periodicity for the bright fringes can be obtained simply by changing the repetition ratio between Sr-rich and La-rich planes. But also interestingly enough, the images shown in figure 4 are very similar to those reported by Mori *et al* for $La_{1-x}Ca_xMnO_3$, and are attributed to charge stripes [28]. Another possibility would be that the observation of these bright fringes is giving evidence for the formation of a charge pattern, similar to the one reported for the manganites, for which the amount of ferromagnetic phase depends also on the thermal history of the sample [29].

It must be noticed that no superstructure spots were detected in any of the various crystallites selected and oriented along different zone axes. Moreover, high resolution neutron

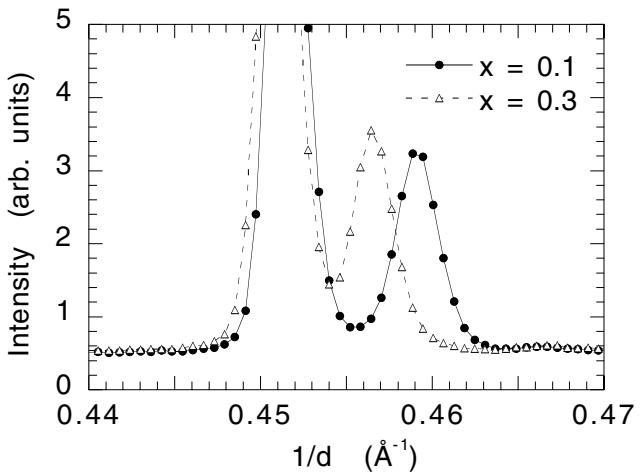

Figure 6. Selected region of the neutron diffraction pattern recorded at 15 K for the $x = 0.10$ and $x = 0.30$ samples annealed at 1273 K; d is the lattice spacing and the lines are the Rietveld profiles that best fit the whole diffraction pattern.

diffraction measurements seems to exclude the coexistence of distinct phases with different chemical composition. Indeed, with increasing x, the volume of the unit cell expands sharply in the range $0 \leqslant x \leqslant 0.1$, and increases linearly with x, for $x > 0.1$. As a result of this expansion, and the decrease of the rhombohedral distortion, the neutron diffraction patterns for $La_{1-x}Sr_xCoO_3$ compounds differ from one another for different values of x. As an example, we show in figure 6 a selected angular region of the neutron diffractograms recorded for the $x = 0.10$ and $x = 0.30$ samples annealed at 1273 K. The solid line is the Rietveld profile, which best reproduces the experimental data in the whole spanned angular range [22]. The peaks corresponding to the two compositions are well separated. The presence of a large amount of an $x \geqslant 0.3$ phase (more than 20%) in the $x = 0.10$ sample, as suggested in [25], would therefore be easily detected. On the contrary, neither extra peaks nor broadening of the Bragg lines have been observed. Of course, the presence of small Sr-rich clusters extended over 10–20 Å would not be detected by such an experiment.

4. Discussion

Where the critical temperature for segregation of a localized-electron and an itinerant-electron phase is too low for atomic diffusion, phase segregation may be accomplished by atomic displacements. In transition-metal AMO_3 oxides with the perovskite structure, an oxygen displacement within a $(180^\circ - \phi)$ M–O–M bond introduces a shorter M–O bond on one side and a longer one on the other. Cooperative oxygen displacements can segregate domains with shorter metal–oxygen bonds from those with longer bonds. In a mixed-valent system, higher oxidation states are stabilized in the domains with shorter M–O bonds [30]. In this way an electronic phase separation is accomplished without the introduction of the chemical inhomogeneities that characterize a conventional phase segregation by atomic diffusion. Such a situation has been suggested [30] to be responsible for the CMR phenomenon in the manganese-oxide perovskites and, we argue, could explain the magnetic behaviour of Sr doped $LaCoO_3$. The phase segregation would allow the phase boundaries to be mobile. Where one phase is ferromagnetic with a Curie temperature significantly higher than the other phase, superparamagnetic clusters may be stabilized above the long-range ordering temperature T_C of the matrix and spin–glass behaviour may be found below T_C, in the absence of any measurable chemical inhomogeneity.

The cooperative oxygen displacements can be dynamic. In that case, the oxygen vibrational modes would be correlated to the e_g electron configuration, as the Jahn–Teller electronic ordering is fast, relative to the atomic vibrations. As pointed out by Goodenough *et al* for gallium doped manganites [31], the coupling of the vibrational modes and the e_g configuration affects the interatomic spin–spin interactions and the transport properties of the system. The existence of vibronic electronic states in Ca-doped manganites has been confirmed by measurements of the thermoelectric power in $^{18}O/^{16}O$ isotope-exchanged samples [32]. In this vibronic phase, trapped polarons form extended hole-rich domains, as in a mobile charge-density wave [32].

Substitution of Sr^{2+} for La^{3+} in $LaCoO_3$ oxidizes the CoO_3 array. The origin of the ferromagnetic interactions in Sr doped $LaCoO_3$ seems to be the double exchange mechanism [33] between Co^{3+} and Co^{4+}, analogous to the parent manganites [34, 35]. However there are some differences with respect to them, as revealed in investigations of mixed Mn–Co perovskites [12] and in measurements of critical exponents at T_C [36]. Antiferromagnetic interactions have been attributed to superexchange interactions between Co^{4+}–Co^{4+} and high-spin Co^{3+}–Co^{3+} [23], or to a long-range Ruderman–Kittel–Kasuya–Yosida (RKKY)-type interaction between Co^{4+}–Co^{4+}, whose magnitude and sign would depend on the distance

between the involved ions [17], like in common SG systems [37, 38].

If the concentration of dopants in a double-exchange system is increased, a phase segregation can take place [39]. The Co(IV) : t^5e^0 ions are in a low-spin state, and the stronger Co(IV)–O covalent bonding stabilizes, to the lowest temperatures, an intermediate-spin state ($S = 1$, t^5e^1) at neighbouring trivalent cobalt sites. The antibonding e^1 electrons are shared with the Co(IV) ions within an IS molecular-orbital cluster and couple the localized t^5 configurations ferromagnetically. Below a critical temperature T_C, the clusters become superparamagnetic within a Co^{3+}-ion matrix, in which the IS configurations remain localized and paramagnetic. A strong deviation of the high-temperature magnetic susceptibility from the Curie–Weiss behaviour (for samples with $x > 0.2$) indicates that the system enters into a cluster-fluctuation regime below about 300 K [26]. Evidence for a dynamic phase separation, where manganese clusters oscillate between a ferromagnetic metallic phase and a non-magnetic phase with higher electrical resistance, has recently been obtained in $La_{2/3}Ca_{1/3}MnO_3$ [40]. A similar situation could occur in $La_{1-x}Sr_xCoO_3$. However, the techniques we used for our study do not allow us to address this aspect.

The occurrence of a long-range ferromagnetic order corresponds to a percolation threshold for IS metallic clusters. However, the observation by neutron diffraction of a ferromagnetic spin-correlation length of several hundreds of angstroms, even for Sr doping as low as $x = 0.10$, indicates the presence of regions where ferromagnetic coupling is occurring before the percolation threshold is reached. We suggest that for $x \leqslant 0.2$ and low T_a, these regions are formed by interconnected magnetic clusters. The net magnetic moment is eliminated if the interconnecting paths are suppressed, and this can occur upon an increase of T_a due to a charge-carrier redistribution. The onset of the magnetic susceptibility around 240 K would therefore indicate the development of spin correlation inside regions with interconnected clusters, whilst the anomaly observed below 60 K would signal the freezing of the isolated cluster moments. The cluster phase has a peculiar dynamic behaviour, with an ageing effect in the time relaxation of dc magnetization [41]. We have recently observed that this ageing effect takes place not only below the peak temperature in ZFC dc magnetization, but also at any temperature below T_C. This indicates a collective dynamics of the ensemble of interacting cluster moments, which progressively block with decreasing temperature before freezing together at about 60 K.

By increasing the annealing temperature, a charge-carrier redistribution takes place. The 'stripe-like' regions tend to disappear, and ferromagnetism is confined inside the small clusters. The system behaves as a cluster-glass for $0.1 < x < 0.2$ or as a spin–glass for even smaller values of x. Indeed the set-up of a spin–glass phase needs good diffusion of the dopants in order to guarantee randomness and avoid correlations in the impurity positions [38]. This condition seems to be realized only for samples annealed at a sufficiently high temperature. For Sr content larger than $x = 0.20$, the system enters a 'disordered' ferromagnetic phase below T_C. However, ferromagnetism can now be achieved even in the IS matrix, and the disappearance of the stripe-like regions with increasing annealing temperature is accompanied by a magnetic behaviour approaching that of a normal ferromagnetic material.

References

[1] von Helmolt R, Wecker J, Holzapfel B, Schultz L and Samwer K 1993 *Phys. Rev. Lett.* **71** 233
[2] Jin S, Tiefel T H, McCormack M, Fastnacht R R, Ramesh R and Chen L H 1994 *Science* **264** 413
[3] Uehara M, Mori S, Chen C H and Cheong S-W 1999 *Nature* **400** 405
[4] Merithew R D, Weismann M B, Hess F M, Spradling P D, Nowak E R, O'Donnell J, Eckstein J N, Tokura Y and Tomioka Y 2000 *Phys. Rev. Lett.* **84** 3442
[5] Podzorov V, Uehara M, Gershenson M E, Koo T Y and Cheong S-W 2000 *Phys. Rev.* B **61** R3784
[6] Kapusta Cz, Riedi P C, Sikora M and Ibarra M R 2000 *Phys. Rev. Lett.* **84** 4216

[7] Moreo A, Mayr M, Feiguin A, Yunoki S and Dagotto E 2000 *Phys. Rev. Lett.* **84** 5568
[8] Raccah P M and Goodenough J B 1967 *Phys. Rev.* **155** 932
[9] Menyuk N, Dwight K and Raccah P M 1967 *J. Phys. Chem. Solids* **28** 599
[10] Señarís-Rodríguez M A and Goodenough J B 1995 *J. Solid State Chem.* **116** 224
[11] Señarís-Rodríguez M A and Goodenough J B 1995 *J. Solid State Chem.* **118** 323
[12] Gayathri N, Raychaudhuri A K, Tiwary S K, Gundakaram R, Arulraj A and Rao C N R 1997 *Phys. Rev.* B **56** 1345
[13] Saitoh T, Mizokawa T, Fujimori A, Abbate M, Takeda Y and Takano M 1997 *Phys. Rev.* B **56** 1290
[14] Munakata F, Takahashi H, Akimune Y, Shichi Y, Tanimura M, Inove Y, Itti R and Koyama Y 1997 *Phys. Rev.* B **56** 979
[15] Saitoh T, Mizokawa T, Fujimori A, Abbate M, Takeda Y and Takano M 1997 *Phys. Rev.* B **55** 4257
[16] Korotin M A, Ezhov S Yu, Solovyev I V, Anisimov V I, Khomskii D I and Sawatzky G A 1996 *Phys. Rev.* B **54** 5309
[17] Asai K, Yokokura O, Nishimori N, Chou H, Tranquada J M, Shirane G, Higuchi S, Okajima Y and Kohn K 1994 *Phys. Rev.* B **50** 3025
[18] Mahendiran R and Raychaudhuri A K 1996 *Phys. Rev.* B **54** 16044
[19] Golovanov V, Mihaly L and Moodenbaugh A R 1996 *Phys. Rev.* B **53** 8207
[20] Jonker G H and van Santen J H 1953 *Physica* **19** 120
[21] Goodenough J B 1971 *Mater. Res. Bull.* **6** 967
[22] Caciuffo R, Rinaldi D, Barucca G, Mira J, Rivas J, Señarís-Rodríguez M A, Radaelli P G, Fiorani D and Goodenough J B 1999 *Phys. Rev.* B **59** 1068
[23] Itoh M, Natori I, Kubota S and Motoya K 1994 *J. Phys. Soc. Japan* **63** 1486
[24] Mira J, Rivas J, Sánchez R D, Señarís-Rodríguez M A, Fiorani D, Rinaldi D and Caciuffo R 1997 *J. Appl. Phys.* **81** 5753
[25] Anil Kumar P S, Joy P A and Date S K 1998 *J. Appl. Phys.* **83** 7375
[26] Caciuffo R, Mira J, Rivas J, Señarís-Rodríguez M A, Radaelli P G, Carsughi F, Fiorani D and Goodenough J B 1999 *Europhys. Lett.* **45** 399
[27] Stadelmann P A 1987 *Ultramicroscopy* **21** 131
[28] Mori S, Chen C H and Cheong S-W 1998 *Nature* **392** 473
[29] Mathur N 1999 *Nature* **400** 405
[30] Goodenough J B and Zhou J-S 1998 *Materials for Electrochemical Energy Storage and Conversion II*, *MRS Symposia Proceedings No 47Y* ed by D S Gingley, D M Scrosati, T Takamura and Z Zhang, (Pittsburgh, PA: Materials Research Society)
[31] Goodenough J B, Wold A, Arnott R J and Menyuk N 1961 *Phys. Rev.* **124** 373
[32] Zhou J S and Goodenough J B 1998 *Phys. Rev. Lett.* **80** 2665
[33] Zener C 1951 *Phys. Rev.* **82** 403
[34] Anderson P W and Hasegawa H 1955 *Phys. Rev.* **100** 675
[35] de Gennes P G 1960 *Phys. Rev.* **118** 141
[36] Mira J, Rivas J, Vázquez M, García-Beneytez J M, Arcas J, Sánchez R D and Señarís-Rodríguez M A 1999 *Phys. Rev.* B **59** 123
[37] Binder K and Young A P 1986 *Rev. Mod. Phys.* **58** 801
[38] Fischer K H and Hertz J A 1991 *Spin Glasses* (Cambridge: Cambridge University Press)
[39] Arovas D P, Gómez-Santos G and Guinea F 1999 *Phys. Rev.* B **59** 13569
[40] Raquet B, Anane A, Wirth S, Xiong P and von Molnár S 2000 *Phys. Rev. Lett.* **84** 4485
[41] Mira J, Rivas J, Jonason K, Nordblad P, Breijo M P and Señarís-Rodríguez M A 1999 *J. Magn. Magn. Mater.* **196–197** 487